Deficiency of the Cyclin Kinase Inhibitor p21(WAF-1/CIP-1) Promotes Apoptosis of Activated/Memory T Cells and Inhibits Spontaneous Systemic Autoimmunity

Brian R. Lawson,[1] Roberto Baccala,[1] Jianxun Song,[2] Michael Croft,[2] Dwight H. Kono,[1] and Argyrios N. Theofilopoulos[1]

[1]*Department of Immunology, The Scripps Research Institute, La Jolla, CA 92037*
[2]*Division of Immunochemistry, La Jolla Institute for Allergy and Immunology, San Diego, CA 92121*

Abstract

A characteristic feature of systemic lupus erythematosus is the accumulation of activated/memory T and B cells. These G_0/G_1-arrested cells express high levels of cyclin-dependent kinase inhibitors such as p21, are resistant to proliferation and apoptosis, and produce large amounts of proinflammatory cytokines. Herein, we show that ablation of p21 in lupus-prone mice allows these cells to reenter the cell cycle and undergo apoptosis, leading to autoimmune disease reduction. Absence of p21 resulted in enhanced Fas/FasL-mediated activation-induced T cell death, increased activation of procaspases 8 and 3, and loss of mitochondrial transmembrane potential. Increased apoptosis was also associated with p53 up-regulation and a modest shift in the ratio of Bax/Bcl-2 toward the proapoptotic Bax. Proliferation and apoptosis of B cells were also increased in $p21^{-/-}$ lupus mice. Thus, modulation of the cell cycle pathway may be a novel approach to reduce apoptosis-resistant pathogenic lymphocytes and to ameliorate systemic autoimmunity.

Key words: CDKI • lupus • replicative senescence • Fas/FasL • cell cycle

Introduction

Foreign antigen-directed immune responses typically involve a sequence of T and B cell activation, clonal expansion, differentiation into effector cells, and, to maintain homeostasis, apoptosis (1, 2). The fraction (~5%) that escapes apoptosis constitutes the self-renewing, long-lived memory population. Autoimmune responses are not as clearly defined in this regard, although similar principles seem to govern antigen presentation, costimulation, and cytokine requirements (3). However, differences in the kinetics and homeostatic mechanisms must exist because self-antigens are continually present, and alterations in lymphocyte functions and phenotypes are observed with autoimmune disease progression.

A common feature of lupus-prone mice is the marked accumulation of activated/memory phenotype ($CD44^{hi}$) $CD4^+$ T cells resistant to proliferation and apoptosis (4, 5). Notably, such cells are arrested in the G_0/G_1-phase of the cell cycle and express high levels of certain cyclin-dependent kinase inhibitors (CDKIs), including $p21^{WAF\text{-}1/CIP\text{-}1}$ (5), characteristics that are also associated with replicative senescence (6–8). We hypothesized (5) that repeated stimulation of self-reactive T cells might lead to a state akin to "replicative senescence," wherein T cells no longer cycle, but persist and transcribe autoimmunity-promoting genes such as those encoding proinflammatory cytokines (9). A similar accumulation of activated B cells resistant to proliferation and apoptosis is also found in lupus-prone strains (10–13).

Although cell cycle and apoptosis are opposing biologic phenomena, studies have shown that they are interconnected (14, 15). TCR-, mitogen-, and superantigen-mediated apoptosis of mature T cells requires an initial progression through several cellular divisions (16–18). Furthermore, blocking cyclin B with antisense (AS) oligonucleotides inhibits TCR signal–mediated apoptosis (19). Thus, cell cycle blockade at the G_0/G_1-phase could be a major factor in apoptosis resistance and accumulation of activated/memory phenotype T cells in systemic autoimmunity.

Cell cycle progression is controlled by several proteins, including cyclins, cyclin-dependent kinases (CDKs), and CDKIs (15, 20). CDKIs are negative regulators of cyclin–

Address correspondence to Argyrios N. Theofilopoulos, Dept. of Immunology, The Scripps Research Institute, 10550 N. Torrey Pines Rd/IMM3, La Jolla, CA 92037. Phone: (858) 784-8135; Fax: (858) 784-8361; email: argyrio@scripps.edu

Abbreviations used in this paper: AICD, activation-induced cell death; AS, antisense; BrdU, bromodeoxyuridine; CDK, cyclin-dependent kinase; CDKI, cyclin-dependent kinase inhibitor; GN, glomerulonephritis; KLH, keyhole limpet hemocyanin; MAPK, mitogen-activated protein kinase; TNP, trinitrophenyl; TD, T-dependent.

J. Exp. Med. © The Rockefeller University Press • 0022-1007/2004/02/547/11 $8.00
Volume 199, Number 4, February 16, 2004 547–557
http://www.jem.org/cgi/doi/10.1084/jem.20031685

CDK complexes and, based on structural and functional characteristics, have been grouped into two distinct families, Ink4 and Cip/Kip (20, 21). The Ink4 proteins ($p16^{INK4A}$, $p15^{INK4B}$, $p18^{INK4C}$, and $p19^{INK4D}$) form binary complexes with CDK4 and CDK6 and block the G_1 to S phase transition. In contrast, the pancyclin Cip/Kip proteins ($p21^{CIP-1}$, $p27^{KIP1}$, and $p57^{KIP2}$) bind to the entire cyclin/CDK holoenzymes, inhibiting transitions at all stages of the cell cycle. Among the CDKIs, p21 is likely to play a prominent role in both cell cycle and apoptosis by promoting G_1-arrest, inhibiting proliferating cell nuclear antigen, affecting key players in the apoptotic machinery (such as p53 and procaspase 3), and contributing to cellular senescence (21–24). The induction of p21 by several growth factors and cytokines, including IFN-γ, has also been reported (25, 26). Surprisingly, despite the multiple roles ascribed to this CDKI and the wide range of cells expressing this gene during development and cellular activation (21), p21-deleted mice develop normally at least up to 7 mo of age (27).

In light of this, we reasoned that absence of p21 might release repeatedly activated, self-reactive T and B cells from their replication/apoptosis-resistant state, allowing their entry into the S phase and subsequent apoptosis, thus reducing their accumulation and presumptive pathogenicity in systemic autoimmunity. Herein, we report that homozygous deletion of the *p21* gene indeed reduced serologic, cellular, and histologic disease manifestations and increased survival of male BXSB lupus-prone mice. This resistance to autoimmunity appeared to be primarily due to an increased susceptibility of activated/memory phenotype T and B cells to activation-induced cell death (AICD).

Materials and Methods

Mice. $p21^{-/-}$ mice, obtained from P. Leder (Harvard Medical School, Boston, MA), were backcrossed to the BXSB strain. Only male $p21^{+/+}$ and $p21^{-/-}$ littermates were compared with survival, serologic, and histopathologic data compiled from mice at generations 7–11, and in vitro data from generations 10–13.

Flow Cytometry. Cells were stained with antibodies to CD4, CD5, CD8, CD11b, CD19, B220, CD21, CD23, CD25, CD27, CD44, CD69, IgM, IgD, Annexin V, Fas, FasL, TCRα/β, IFN-γ, or PI (all obtained from BD Biosciences). Data were acquired on a FACS Calibur™ and analyzed with CELLQuest™ software (Becton Dickinson).

Proliferation and Apoptosis Assays. In vitro studies were conducted with cells from 1–2-mo-old mice, an age at which frequencies and phenotypes of T and B cell subsets were equivalent between the two genotypes. LN cells were incubated with 5 μg/ml of soluble anti-CD28 and increasing concentrations of plate-bound anti-CD3 (BD Biosciences) for 48 h. [^{3}H]thymidine (1 μCi) incorporation was measured 15 h later. Subsequently, the optimum coating concentration was selected (10 μg/ml of anti-CD3), and LN cells were plated on anti-CD3–coated plates plus 5 μg/ml of soluble anti-CD28, and analyzed for [^{3}H]thymidine incorporation every 24 h for 6 d (28). B cells were activated with 10 μg/ml of soluble goat $F(ab')_2$ anti–mouse IgM (Jackson ImmunoResearch Laboratories) and IL-4. [^{3}H]Thymidine incorporation was measured every 24 h for 3 d. In vivo proliferation of splenic T and B cells was determined by long-term bromodeoxyuridine (BrdU) incorporation (29). In brief, BrdU was administered in drinking water for 9 d (0.8 mg/ml), made fresh daily. After BrdU labeling, splenocytes were analyzed by FACS® using the BrdU Flow kit (BD Biosciences) according to the manufacturer's instructions.

To assess T cell AICD, LN cells were cultured for 48 h with 0.5 μg/ml of soluble anti-CD3 and religated with 10 μg/ml of plate-bound anti-CD3 (BD Biosciences; reference 18). To block AICD, anti-FasL antibody (BD Biosciences) or soluble Fas/Fc (a gift from D. Green, La Jolla Institute for Allergy and Immunology, San Diego, CA) was added at 10 μg/ml, whereas anti-Fas antibody (BD Biosciences) was added at 5 μg/ml to induce AICD. For B cell apoptosis, splenocytes were incubated with 10 μg/ml of soluble goat $F(ab')_2$ anti–mouse IgM.

T and B cells undergoing apoptosis were stained at 24-h intervals with either anti-CD4, anti-CD8, or anti-CD19, plus Annexin V and PI. The percentage of Annexin V^+/PI^- T or B cells was determined by FACS®. Loss of mitochondrial transmembrane potential was determined using the JC-1 mitochondrial transmembrane potential ($\Delta\Psi m$) detection kit (Cell Technology, Inc.) according to the manufacturer's instructions. Conversion of procaspases 8 and 3 to active caspases was assessed by the APO LOGIX carboxyfluorescein caspase detection kit and APO ACTIVE 3 antibody detection kit (Cell Technology, Inc.), respectively.

RNase Protection Assay. RNase protection assay of p21 expression on sorted $CD19^+$ B cells was performed as described previously (5). In brief, riboprobes for p21 and L32 (housekeeping gene) were prepared and labeled with α-[^{32}P]UTP (Riboprobe System; Promega). Purified probes were hybridized to 5 μg of total B cell RNA (RPA Kit I; Torrey Pines Biolabs), protected products were run on a 6% polyacrylamide sequencing gel, and bands were revealed by overnight exposure on autoradiographic film (Eastman Kodak Co.).

Stem and T Cell Cycling. Bone marrow cells from 1-mo-old and LN T cells from 3-mo-old male BXSB $p21^{+/+}$ or $p21^{-/-}$ mice (n = 4 mice/group) were stained with either a mouse lineage panel and anti–Sca-1 (both obtained from BD Biosciences), or anti-CD4 and anti-CD44. Cells were analyzed by FACS® after surface immunophenotyping and sequential incubation with 1.67 μM of DNA-binding dye Hoechst 33342 (Molecular Probes) and 1 μg/ml of RNA-binding dye Pyronin Y (Sigma-Aldrich; reference 30).

AS Assays. LN cells from 2-mo-old wild-type BXSB male mice were activated with plate-bound anti-CD3 or religated to induce apoptosis, as aforementioned, in the presence of 400 nM of either of two Penetratin-1–coupled p21-specific phosphorothioated AS oligonucleotides: p21AS no. 1, 5′-ACATCACCAGGATTGGACAT-3′ (31); and p21AS no. 2, 5′-TGTCAGGCTGGTCTGCCTCC-3′ (32) or a similarly processed control oligonucleotide obtained from Qbiogene: control AS, 5′-TGGATCCGACATGTCAGA-3′ (32).

Western Blots. Wild-type and $p21^{-/-}$ BXSB T cells were activated with 10 μg/ml anti-CD3 plus 5 μg/ml anti-CD28 and analyzed for p21, Bax, Bcl-2, and p53 protein expression. In brief, lysates were prepared from 2.0×10^7 cells, and protein was measured by microprotein assay (Bio-Rad Laboratories). Proteins were separated on a 15% SDS-PAGE (Bio-Rad Laboratories), transferred to polyvinyl difluoride membrane (Immobilon-P; Millipore), and blocked with 5% milk powder in PBS. After overnight incubation at 4°C with primary antibodies to p21, Bax, Bcl-2, or p53, proteins were revealed with appropriate horseradish peroxidase–conjugated secondary antibodies (BD Biosciences or Santa Cruz Biotechnology, Inc.) followed by SuperSignal

chemiluminescence (Pierce Chemical Co.). Radiographs were scanned on the Personal Densitometer SI and analyzed by ImageQuant 4.2a (both Amersham Biosciences).

T-dependent (TD) Responses. Mice were injected s.c. with 100 μg trinitrophenyl (TNP)–keyhole limpet hemocyanin (KLH; Biosearch Technologies) emulsified in CFA. Secondary responses were assessed by a s.c. boost of 100 μg TNP-KLH in saline on day 21. Mice were bled at the indicated times, and antibody levels were determined by ELISA (33).

Serologic Analysis. Total and antichromatin serum IgG subclasses were measured by ELISA using 96-well plates coated with goat anti–mouse IgG (Jackson ImmunoResearch Laboratories) or mouse chromatin (29). Bound IgG subclasses were detected using AP-conjugated IgG subclass-specific antibodies (Caltag). Standard curves for each subclass were generated using calibrated mouse serum (Accurate Chemical and Scientific Company).

Kidney Disease. AZOSTIX strips (Bayer) were used to measure blood urea nitrogen and graded on a 1–4 scale (1 = 5–15, 2 = 15–26, 3 =30–40, and 4 = 50–90 mg/dl). Histologic examination of periodic-acid Schiff–stained kidneys was done in a blind manner at 4 mo of age, and severity of glomerulonephritis (GN) was defined on a scale of 0–4 (34). For immunohistology, frozen kidney sections were fixed in ice-cold acetone, blocked, and incubated with anti–IgG-FITC (Vector Laboratories); deposits were scored as described previously (29).

Statistics. The Student's *t* test was used for group mean comparisons, and survival was analyzed by the Kaplan-Meier method with comparisons by log-rank test. P-values <0.05 were considered significant.

Results

To examine the role of p21 in systemic autoimmunity, we generated congenic $p21^{-/-}$ lupus-susceptible BXSB mice and assessed disease manifestations, immune homeostasis, and the responses of T and B cells. Males were exclusively studied because severe early life lupuslike disease in this strain requires the *Yaa* (Y chromosome accelerator of autoimmunity and lymphoproliferation) susceptibility gene (13).

Reduced Hypergammaglobulinemia and Autoantibodies in $p21^{-/-}$ BXSB Mice. Initial studies were performed to determine the effects of p21 deficiency on autoimmune manifestations. Control mice exhibited typical hypergammaglobulinemia at 4 mo of age, whereas all IgG subclasses were significantly lower in $p21^{-/-}$ littermates, approaching levels seen in C57BL/6 normal mice (Fig. 1 a). Antichromatin levels, predominantly of the IgG2a subclass, were also high in the wild-type littermates. In contrast, antichromatin autoantibodies of all subclasses were greatly reduced in the $p21^{-/-}$ mice (Fig. 1 b).

Enhanced Survival and Reduced Kidney Disease in $p21^{-/-}$ BXSB Mice. The mortality and immunopathology of the control $p21^{+/+}$ littermates were similar to those of our male BXSB colony, indicating sufficient backcrossing of the major BXSB lupus susceptibility genes. In contrast, there was a dramatic reduction in mortality and GN in BXSB $p21^{-/-}$ mice. Control BXSB males showed 50% mortality at 5.6 mo and 100% mortality by 6.3 mo, whereas ~80% of $p21^{-/-}$ mice were alive at 13 mo and ~65% at 16.5 mo (Fig. 1 c). GN (2.1 ± 0.4 vs. 3.4 ± 0.2; $P < 0.05$), IgG deposit scores (1.5 ± 0.2 vs. 3.1 ± 0.4; $P < 0.05$) (Fig. 1 d), and blood urea nitrogen levels (1.1 ± 0.1 vs. 3.2 ± 0.2; $P < 0.05$) were also significantly reduced in 4-mo-old BXSB $p21^{-/-}$ mice. Thus, p21 is clearly essential for the accelerated lupus in BXSB mice.

Fewer Total and Activated/Memory T and B Cells in $p21^{-/-}$ BXSB Mice. The effects of p21 deficiency on in vivo autoimmune T and B cell homeostasis, proliferation, and apoptosis were examined. The weights and cellular compo-

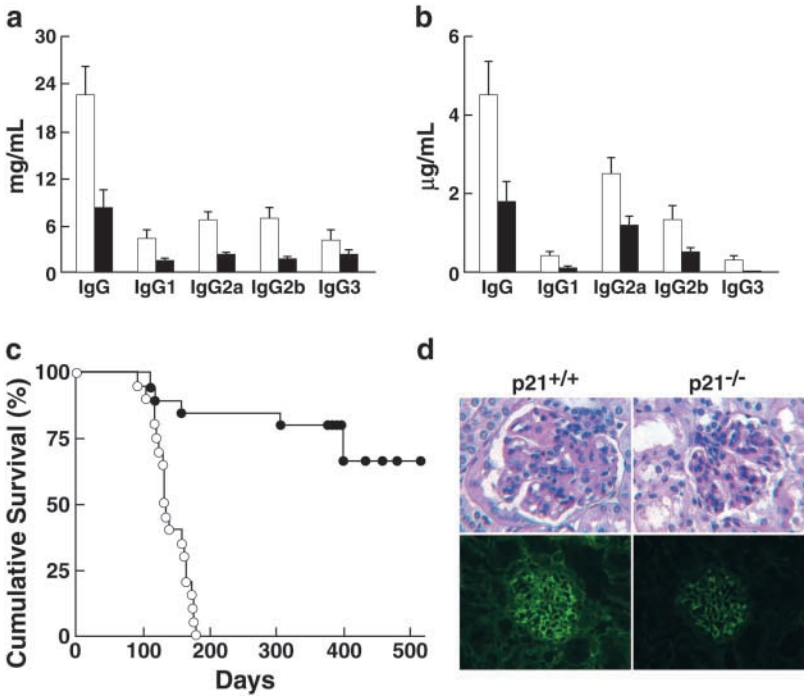

Figure 1. Decreased autoimmune disease in male $p21^{-/-}$ BXSB mice. (a and b) Reduced serum polyclonal (left) and antichromatin (right) IgG subclasses in 4-mo-old male BXSB $p21^{-/-}$ mice ($n = 8$ mice/group; mean ± SEM). (shaded bars) BXSB $p21^{-/-}$ mice. (unshaded bars) $p21^{+/+}$ BXSB mice. For all polyclonal and antichromatin total and subclass IgG levels, $P < 0.05$ for $p21^{-/-}$ versus $p21^{+/+}$. (c) Increased cumulative survival rates of $p21^{-/-}$ BXSB mice ($P < 0.0001$). Male BXSB $p21^{+/+}$ ($n = 16$) and $p21^{-/-}$ ($n = 15$) littermates were followed for up to 500 d. (●) BXSB $p21^{-/-}$ mice. (○) BXSB $p21^{+/+}$ mice. (d) Glomerular pathology (top) and IgG deposits (bottom) of representative 4-mo-old $p21^{+/+}$ and $p21^{-/-}$ mice. Increased segmental mesangial proliferation and accumulation of periodic-acid Schiff–positive mesangial matrix material were seen in $p21^{+/+}$ mice, whereas $p21^{-/-}$ mice exhibited significantly less glomerular damage, as well as decreased segmental granular mesangial and capillary wall deposits of IgG (top, 630×; bottom, 400×).

Table I. *Spleen and LN Analysis of BXSB p21$^{-/-}$ Mice*

	Weight	Total ($\times 10^6$)	T cells ($\times 10^6$)							B cells ($\times 10^6$)	
			CD4$^+$	CD4$^+$CD44^{hi}	CD4$^+$CD44^{hi}AV$^+$	CD4$^+$IFN-γ^+	CD8$^+$	CD8$^+$CD44^{hi}	CD8$^+$CD44^{hi}AV$^+$	CD19$^+$	CD19$^+$CD69$^+$
Spleen											
BXSB p21$^{+/+}$	0.4 ± 0.05	190.4 ± 21.0	29.4 ± 4.4	24.4 ± 3.3	0.97 ± 0.02 (4%)[a]	ND	15.3 ± 8.0	8.8 ± 4.6	ND	126 ± 14.4	9.1 ± 2.2
BXSB p21$^{-/-}$	0.3 ± 0.1	170.4 ± 37.1	18 ± 2.2[b]	11.7 ± 1.4[b]	1.91 ± 0.03[b] (16%)[a]	ND	14.5 ± 1.5	6.7 ± 0.4	ND	102.7 ± 20.5	6.0 ± 1.3
LN											
BXSB p21$^{+/+}$	0.5 ± 0.11	249.2 ± 21.0	75.6 ± 9.9	45.1 ± 6.4	3.7 ± 0.2 (8%)[a]	16.6 ± 2.2	25.3 ± 5.0	14.8 ± 2.6	2.2 ± 0.6	117.8 ± 2.5	5.3 ± 1.9
BXSB p21$^{-/-}$	0.1 ± 0.04[b]	52 ± 4.7[b]	15.3 ± 3.2[b]	6.5 ± 0.2[b]	1.4 ± 0.1[b] (22%)[a]	3.7 ± 1.0[b]	4.5 ± 1.5[b]	1.7 ± 0.4[b]	0.4 ± 0.1[b]	27.2 ± 4.1[b]	0.8 ± 0.0.3[b]

Spleen and combined LN (axillary, inguinal, cervical, and mesenteric) weights (n = 8 mice/group) are shown (mean ± SEM g). T and B cell subsets from p21$^{+/+}$ and p21$^{-/-}$ BXSB mice at 4 mo of age are indicated as total numbers (mean ± SEM) of splenocytes or their respective subset (n = 5 mice/group).
[a]Percent of CD4$^+$CD44^{hi} T cells that are AV$^+$.
[b]$P < 0.05$ between p21$^{+/+}$ and p21$^{-/-}$ mice. ND, not determined.

sition of spleen and LN are shown in Table I. Spleen weight and total cell numbers as well as numbers of CD8$^+$ and activated/memory CD8$^+$CD44^{hi} T cells were unaffected by the lack of p21, but, strikingly, total splenic CD4$^+$ and activated/memory CD4$^+$CD44^{hi} cells were significantly reduced ($P < 0.05$). When spleen cells were examined for preapoptotic cells, p21$^{-/-}$ mice had a significant twofold increase in the number of Annexin V–binding CD4$^+$CD44^{hi} T cells, which represented a fourfold increase in percentage (16.3 ± 2.1 vs. 4.0 ± 0.8%; $P < 0.05$; Table I). In contrast, splenic B cells (CD19$^+$), activated (Table I, CD69$^+$), memory (CD27$^+$), B1a (CD5$^+$), follicular, and marginal zone B cell populations (not depicted) were unaffected. BXSB male mice also develop an expanded peripheral blood population of unusual Mac-1$^+$ MHC class II$^-$ monocytes whose contributions to disease remains unknown (35). However, the frequency of these cells was equivalent in p21$^{-/-}$ and p21$^{+/+}$ mice (20.3 ± 1.3 vs. 19.2 ± 2.1%).

For the LN, there were significant approximately fivefold reductions in both weight and total cell numbers in p21$^{-/-}$ mice at 4 mo as well as lower numbers of T and B cells and their subsets (Table I, $P < 0.05$). Notably, the percentage of preapoptotic (Annexin V$^+$) activated/memory CD4$^+$CD44^{hi} T cells was ~2.6-fold higher in the p21$^{-/-}$ versus p21$^{+/+}$ mice (21.5 vs. 8.2%; $P < 0.05$). The absolute number of intracellular IFN-γ^+ T cells was also greatly reduced in LNs of p21-deficient mice (Table I).

Enhanced Cycling of Activated/Memory CD4$^+$CD44^{hi} T Cells in p21$^{-/-}$ BXSB Mice. Analysis of in vivo proliferation indicated enhanced cycling of CD4$^+$ T cells in p21-deficient animals, with significant increases in both total

Table II. *Long-Term In Vivo BrdU Incorporation of T and B Cells in Male BXSB p21$^{+/+}$ and p21$^{-/-}$ Mice*

	BrdU^{hi}	
Cell population	BXSB p21$^{+/+}$	BXSB p21$^{-/-}$
	%	%
CD4$^+$	8.9 ± 0.9	19.0 ± 2.3[a]
CD4$^+$CD44^{hi}	24.2 ± 2.0	36.5 ± 3.2[a]
CD8$^+$	9.7 ± 1.2	15.2 ± 2.4
CD8$^+$CD44^{hi}	13.1 ± 1.8	12.4 ± 2.9
CD45R/B220$^+$	25.5 ± 2.1	29.0 ± 5.8

4-mo-old male BXSB p21$^{+/+}$ and p21$^{-/-}$ were fed BrdU in drinking water for 9 d. T and B cells (B220$^+$) defined by FACS® as BrdU^{hi} are indicated as percentages of the listed cell populations.
[a]$P < 0.05$ between male BXSB p21$^{+/+}$ and p21$^{-/-}$ mice (n = 3).

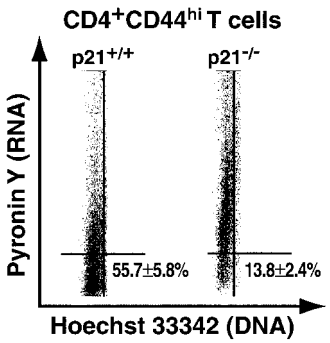

Figure 2. Representative distribution of G_0- versus G_1-phase in CD4$^+$CD44^{hi} T cells. Splenocytes from 3-mo-old mice (n = 4 animals/group) were stained with antibodies to CD4 and CD44, followed by sequential incubation with Hoechst 33342 (DNA-binding dye) and Pyronin Y (RNA-binding dye) and analyzed by flow cytometry. Pyronin Y staining of G_0/G_1-phase CD4$^+$CD44^{hi} T cells from p21$^{-/-}$ and p21$^{+/+}$ BXSB mice is shown ($P < 0.05$).

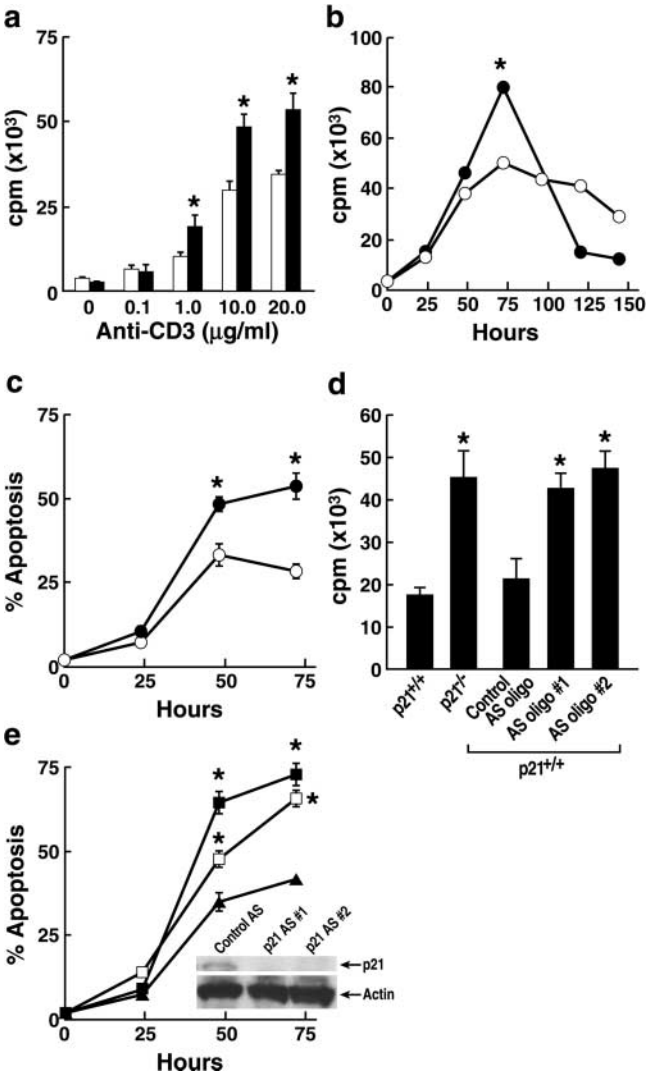

Figure 3. Enhanced proliferation and apoptosis of $p21^{-/-}$ T cells from male BXSB mice. (a) Increased proliferation of $p21^{-/-}$ T cells after in vitro cross-linking of antigen receptors. LN cells (n = 3 mice/group) were stimulated with increasing concentrations of plate-bound anti-CD3 (0.1–20 μg/ml) plus 5 μg/ml of soluble anti-CD28 antibodies and assessed for [^{3}H]thymidine incorporation at 72 h (mean ± SEM cpm). (shaded bars) BXSB $p21^{-/-}$ mice. (unshaded bars) $p21^{+/+}$ BXSB mice. (b) Kinetics of in vitro proliferation. LN cells (n = 3 mice/group) were stimulated with 10 μg/ml of plate-bound anti-CD3 plus 5 μg/ml of soluble anti-CD28 antibodies and assessed for [^{3}H]thymidine incorporation at the indicated time points. Results are representative of two independent experiments (n = 3 mice/group). (●) BXSB $p21^{-/-}$ mice. (○) BXSB $p21^{+/+}$ mice. (c) Increased AICD of $p21^{-/-}$ T cells. T cell were stimulated with 0.5 μg/ml of soluble anti-CD3 for 48 h followed by TCR religation with 10 μg/ml of plate-bound anti-CD3 (n = 3 mice/group). Percent of apoptotic (Annexin V^+PI^-) $CD4^+$ T cells was determined by FACS®. Similar results were obtained with $CD8^+$ T cells. (●) BXSB $p21^{-/-}$ mice. (○) BXSB $p21^{+/+}$ mice. (d) Increased proliferation of wild-type BXSB T cells treated with p21 AS oligonucleotides. LN cells (n = 4 mice/group) were stimulated with 10 μg/ml of plate-bound anti-CD3 plus 5 μg/ml of soluble anti-CD28 antibodies in the presence of either p21 AS or control oligonucleotides (all AS oligonucleotides at 400 nM) and assessed for [^{3}H]thymidine incorporation (mean ± SEM cpm). (e) Increased AICD of wild-type BXSB T cells treated with p21 AS oligonucleotides. Wild-type BXSB T cells were stimulated with 0.5 μg/ml of soluble anti-CD3 followed by TCR religation with 10 μg/ml of plate-bound anti-CD3 in the constant presence of p21 AS or control oligonucleotides (400 nM; n = 3 mice/group). (■) AS oligo no. 1. (□) AS oligo no. 2. (▲) Control oligonucleotide. (e, inset) Western blot analysis of wild-type BXSB T cells treated with either p21 AS or control oligonucleotides. T cells were stimulated with 10 μg/ml anti-CD3 and 5 μg/ml CD28 antibodies in the presence of AS or control oligonucleotides (400 nm). Whole cell lysates were analyzed by Western blot using anti-p21 and antiactin antibodies. *, $P < 0.05$ by Student's t test.

$CD4^+BrdU^{hi}$ and $CD4^+CD44^{hi}BrdU^{hi}$ T cells, whereas frequencies of cycling $CD8^+$ T cells and B cells were unaltered (Table II).

To further define the in vivo cycling characteristics of p21-deficient $CD4^+CD44^{hi}$ T cells, the frequency of cells in G_0- versus G_1-phase was determined by the RNA indicator dye Pyronin Y. Strikingly, the frequency of Pyronin Y^{hi} (G1-phase) $CD4^+CD44^{hi}$ T cells was significantly higher in p21-deficient mice versus BXSB male controls (86.2 ± 2.4% vs. 44.3 ± 5.8%; Fig. 2, $P < 0.05$).

Enhanced Proliferation and Apoptosis of $p21^{-/-}$ T Cells. Previous in vitro analyses with $p21^{-/-}$ T cells from nonautoimmune mice showed increased proliferation compared with wild-type T cells (36, 37). Similarly, BXSB $p21^{-/-}$ T cells showed enhanced proliferation compared with wild-type T cells ($P < 0.05$) after engagement of CD3 and CD28, with no apparent alteration of the TCR-induced activation threshold (Fig. 3 a). Increased proliferation was not attributed to enhanced TCR expression, which was equivalent between the two types of T cells before and after stimulation (unpublished data). These findings were further supported by time-kinetic analysis showing equal proliferation of $p21^{-/-}$ and wild-type T cells up to 24 h, but significantly greater proliferation of $p21^{-/-}$ T cells by 72 h (Fig. 3 b). Interestingly, $p21^{-/-}$ T cell proliferation declined faster than control T cells, reaching baseline levels by ~120 h after stimulation compared with >150 h for the $p21^{+/+}$ cells, suggesting increased apoptosis by the p21-deficient cells.

To test whether $p21^{-/-}$ T cells undergo enhanced apoptosis, we assessed in vitro AICD by incubating these cells for 48 h with soluble anti-CD3, followed by religation with plate-bound anti-CD3 (18). At 24 h after religation, the percentage of Annexin V^+/Propidium $Iodide^-$(AV^+PI^-, preapoptotic) $CD4^+$ T cells was similar for $p21^{-/-}$ and $p21^{+/+}$ cells. However, by 48 h, the $p21^{-/-}$ cells showed a greater percentage of preapoptotic cells, which was more pronounced by 72 h (Fig. 3 c, $P < 0.05$). Similar results were obtained with $CD8^+$ T cells (not depicted).

To confirm that the absence of p21 was responsible for the increased proliferation and apoptosis, the effect of Penetratin-conjugated p21 AS oligonucleotides on T cell proliferation and AICD was assessed. Wild-type T cells transfected with either of two p21-specific AS oligonucleotides, but not with a control oligonucleotide, showed significantly increased proliferation (Fig. 3 d) and apoptosis (Fig. 3 e), approaching the levels of the $p21^{-/-}$ cells ($P < 0.05$). Similar results were observed with $CD8^+$ T cells (unpublished data). The oligonucleotides had no discernible effect on viability, and Western blot analysis confirmed that the two specific p21 AS oligonu-

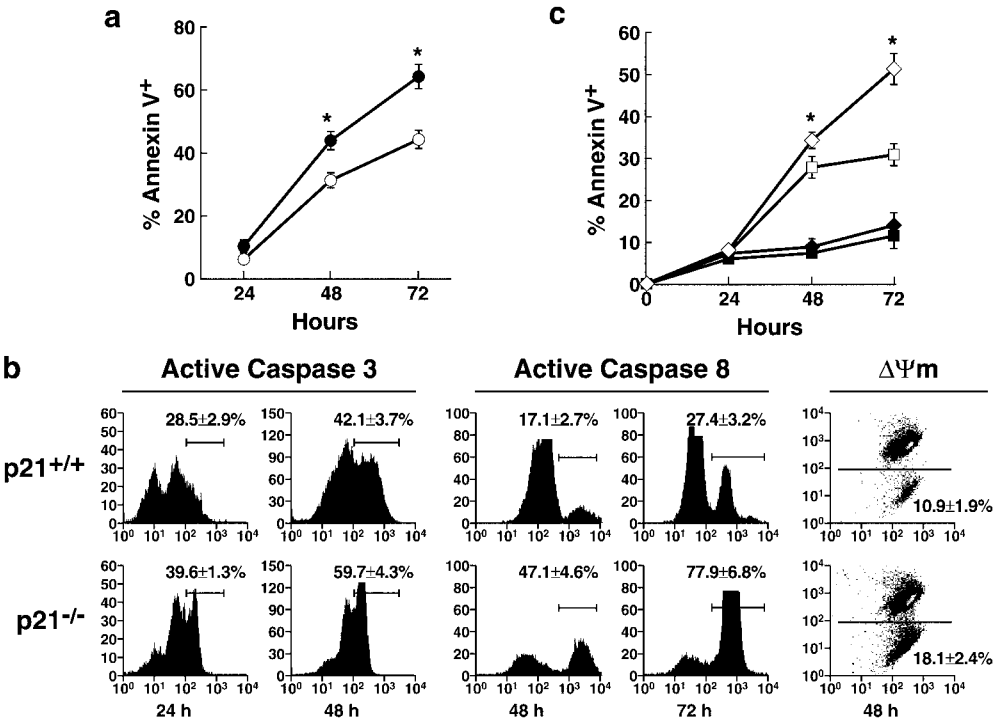

Figure 4. Enhanced Fas/FasL-mediated apoptosis of $p21^{-/-}$ T cells from male BXSB mice. (a) Increased anti-Fas induced apoptosis of $p21^{-/-}$ T cells. LN cells (n = 3 mice/group) were first stimulated with 10 μg/ml of soluble anti-CD3 and 5 μg/ml CD28 for 48 h and then with 5 μg/ml anti-Fas antibody and analyzed for percentage of apoptotic (Annexin V^+PI^-) $CD4^+$ T cells. (●) BXSB $p21^{-/-}$ mice. (○) BXSB $p21^{+/+}$ mice. *, $P < 0.05$. (b) Increased caspase 8 and 3 activation and reduced mitochrondrial membrane potential ($\Delta\Psi m$) in $p21^{-/-}$ T cells after induction of AICD. T cells (n = 3 mice/group) were stimulated with 0.1 μg/ml of soluble anti-CD3, religated with 10 μg/ml of plate-bound anti-CD3, and analyzed by FACS® for activation of caspases 8 and 3 and for change in mitochondrial transmembrane potential. The percentage of cells expressing activated caspases 8 or 3 and reduced $\Delta\Psi m$ is indicated (mean ± SEM). $P < 0.05$ between $p21^{+/+}$ and $p21^{-/-}$ for all time points shown. (c) Fas blockade inhibits AICD of $p21^{+/+}$ and $p21^{-/-}$ T cells. T cells (n = 3 mice/group) were stimulated with 0.1 μg/ml of soluble anti-CD3 for 48 h, religated with 10 μg/ml of plate-bound anti-CD3 in the presence or absence of 10 μg/ml of blocking anti-FasL antibody, and analyzed for Annexin V positivity. Similar inhibition was also observed after treatment with Fas-blocking soluble Fas/Fc. (◆) BXSB $p21^{-/-}$ mice plus anti-FasL. (■) BXSB $p21^{+/+}$ mice plus anti-FasL. (◇) BXSB $p21^{-/-}$ mice. (□) BXSB $p21^{+/+}$ mice. *, $P < 0.05$ for untreated (◇ or □) versus anti-FasL–treated groups (◆ or ■) at 48 and 72 h, and for untreated $p21^{-/-}$ (◇) versus $p21^{+/+}$ (□) mice at 72 h.

cleotides, but not the control oligonucleotide, efficiently blocked p21 protein expression (Fig. 3 e, inset).

Enhancement of the Extrinsic Pathway of Apoptosis in $p21^{-/-}$ T Cells. Fas and FasL expression of anti-CD3– and anti-CD28–activated $p21^{+/+}$ and $p21^{-/-}$ CD4 T cells was equivalent (unpublished data). However, anti-Fas–induced apoptosis of activated CD4 T cells was higher in p21-deficient T cells (Fig. 4 a). Accordingly, kinetic studies showed that the frequency of $p21^{-/-}$ T cells undergoing AICD that had converted initiator procaspase 8 and effector procaspase 3 to active caspases was significantly higher than wild-type cells at all time points (Fig. 4 b). Similarly, loss of mitochondrial transmembrane potential was more pronounced in $p21^{-/-}$ than $p21^{+/+}$ cells (Fig. 4 b). However, AICD was inhibited in both types of T cells by either anti-FasL mAb (Fig. 4 c) or Fas/Fc (not depicted). Thus, as expected, the Fas/FasL pathway is the primary mediator of AICD in $p21^{+/+}$ and $p21^{-/-}$ T cells, but the CD95 signaling cascade and associated events are amplified in $p21^{-/-}$ cells.

Participation of the Intrinsic Pathway of Apoptosis. Although the extrinsic CD95-mediated apoptosis pathway is generally sufficient for AICD, depending on cell type and/or signal strength, the intrinsic pathway may facilitate this process (38–40). $p21^{-/-}$ T cells cultured with anti-CD3 and anti-CD28 for 48 h expressed 1.9-fold more p53 and 1.7-fold less Bcl-2 protein than control cells. Although Bax expression was unaltered, the ratio of Bax/Bcl-2 shifted moderately toward the proapoptotic Bax (5.3 in $p21^{-/-}$ vs. 3.1 in $p21^{+/+}$) (Fig. 5; $P < 0.05$). In addition, activated wild-type T cells cultured in the presence of transfecting p21 AS oligonucleotides showed a 1.7-fold decrease in Bcl-2 and, in this case, a 1.9-fold increase in Bax expression, resulting in a more pronounced shift in the Bax/Bcl-2 ratio (8.1; $P < 0.05$).

Enhanced Proliferation and Apoptosis of $p21^{-/-}$ B Cells. As reported for T cells, B cells from lupus-predisposed mice have also been shown to be both arrested in G_1 and apoptosis resistant (10, 41). Indeed, we detected high p21 levels in male, but not female, B cells (Fig. 6 a). Accordingly, activation with anti-IgM plus IL-4 induced higher proliferation (Fig. 6 b; $P < 0.05$), and cross-linking with anti-IgM resulted in accelerated and enhanced apoptosis of $p21^{-/-}$ compared with wild-type B cells (Fig. 6 c; $P < 0.05$).

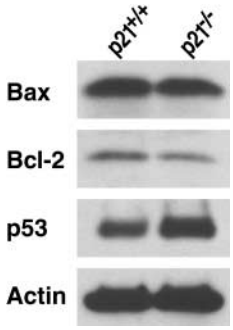

Figure 5. Participation of the intrinsic pathway of apoptosis in $p21^{-/-}$ T cells from male BXSB mice. Increased p53 and reduced Bcl-2 expression in activated $p21^{-/-}$ T cells. T cells (n = 5 mice/group) were activated with 10 μg/ml anti-CD3 plus 5 μg/ml anti-CD28, and lysates were analyzed by Western blot.

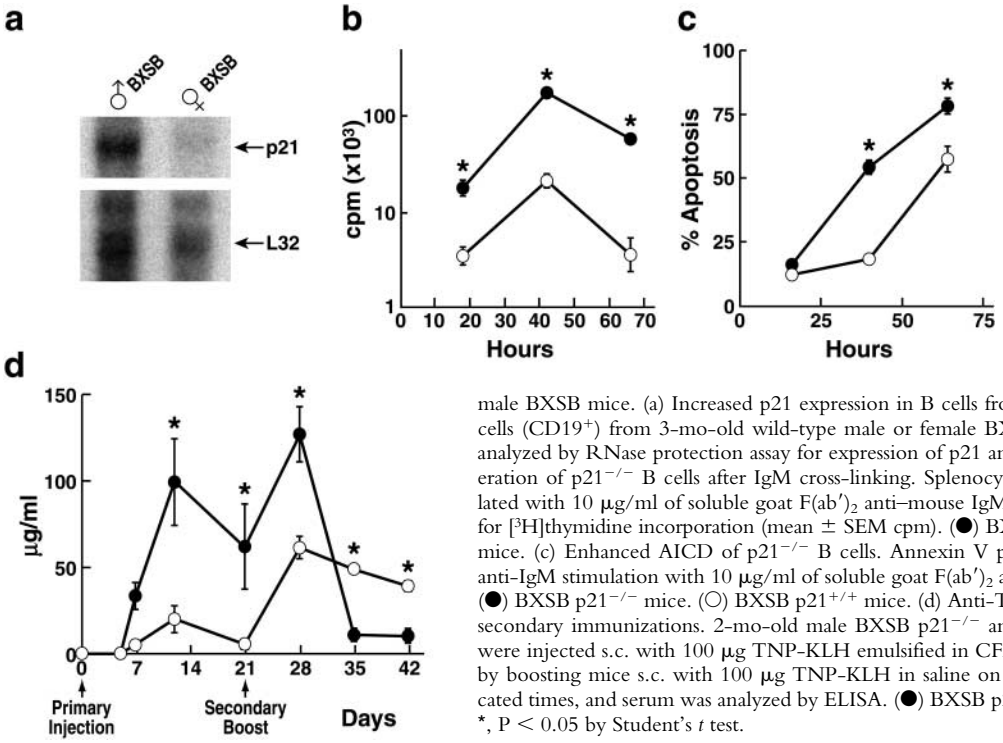

Figure 6. Enhanced proliferation and apoptosis, and reduced late secondary immunoglobulin responses of $p21^{-/-}$ B cells from male BXSB mice. (a) Increased p21 expression in B cells from older male BXSB mice. Sorted B cells ($CD19^+$) from 3-mo-old wild-type male or female BXSB mice ($n = 5$ mice/group) were analyzed by RNase protection assay for expression of p21 and L32 (control). (b) Increased proliferation of $p21^{-/-}$ B cells after IgM cross-linking. Splenocytes ($n = 3$ mice/group) were stimulated with 10 μg/ml of soluble goat $F(ab')_2$ anti–mouse IgM in the presence of IL-4 and assessed for $[^3H]$thymidine incorporation (mean ± SEM cpm). (●) BXSB $p21^{-/-}$ mice. (○) BXSB $p21^{+/+}$ mice. (c) Enhanced AICD of $p21^{-/-}$ B cells. Annexin V positivity of B cells was assessed after anti-IgM stimulation with 10 μg/ml of soluble goat $F(ab')_2$ anti–mouse IgM ($n = 3$ mice/group). (●) BXSB $p21^{-/-}$ mice. (○) BXSB $p21^{+/+}$ mice. (d) Anti-TNP antibody levels after primary and secondary immunizations. 2-mo-old male BXSB $p21^{-/-}$ and $p21^{+/+}$ mice ($n = 4$ mice/group) were injected s.c. with 100 μg TNP-KLH emulsified in CFA. Secondary responses were assessed by boosting mice s.c. with 100 μg TNP-KLH in saline on day 21. Mice were bled at the indicated times, and serum was analyzed by ELISA. (●) BXSB $p21^{-/-}$ mice. (○) BXSB $p21^{+/+}$ mice. *, $P < 0.05$ by Student's *t* test.

Enhanced Primary, but Reduced Late Secondary, TD IgG Responses in $p21^{-/-}$ BXSB Mice. When TD antibody responses to TNP-KLH were examined, $p21^{-/-}$ mice showed fivefold higher primary IgG (Fig. 6 d) and marginally increased IgM (not depicted) responses at day 14 compared with wild-type mice. However, 7 d after rechallenge, the secondary IgG response increased twofold in $p21^{-/-}$ versus 12-fold in the wild-type mice. Notably, the secondary response in the $p21^{-/-}$ mice precipitously declined thereafter to almost baseline levels by day 35, whereas the decline was gradual in the wild-type mice, a finding compatible with enhanced AICD in the $p21^{-/-}$ cells.

Fewer Quiescent Stem Cells in $p21^{-/-}$ BXSB Mice. We also determined whether $p21^{-/-}$ BXSB mice have reduced numbers of quiescent stem cells by analyzing the RNA content of $Lin^-Sca\text{-}1^+$ bone marrow cells using Pyronin Y staining. Similar to previous papers with $p21^{-/-}$ normal background mice (30), autoimmune $p21^{-/-}$ mice had fewer stem cells in G_0-phase than controls (7.8 ± 0.4% vs. 12.2 ± 1.25%; $P < 0.01$), perhaps reducing the renewal capacity of these cells and consequent generation of precursor T and B cells.

Discussion

Herein, we demonstrate that deletion of the CDKI p21 significantly reduced serologic, cellular, and histologic disease manifestations and increased survival of lupus-prone BXSB mice. Furthermore, there was reduced accumulation of proliferation- and apoptosis-resistant T and B cells through a novel mechanism involving enhanced entry of these cells into the cell cycle followed by apoptotic death. These findings clearly show that accumulation of replication/apoptosis-resistant T and B cells in this spontaneous lupus model is dependent on increased p21 expression, and suggest that these cells contribute significantly to the autoimmune and inflammatory processes that are critical for disease pathogenesis.

Classically, p21 inhibits cell cycle entry by blocking formation of active cyclin–CDK complexes. However, more recently identified p21 functions, including inhibition of DNA replication through proliferating cell nuclear antigen binding, repression of E2F, interference with c-Myc, control of certain transcription coactivators, and other interactions may also be involved in cell cycle blockade (21, 24).

Growth factors initiate and maintain the entry of cells from G_1 to S phase in the cell cycle (42). Mitogen-activated protein kinase (MAPK) signaling induces D cyclins, resulting in activation of CDK4 and CDK6, and progression of cells through G_1. However, MAPK signaling has also been shown to induce CDKIs, including p21, and growth arrest (43–45). Thus, it has been suggested that strong or sustained activation of MAPK signaling leads to induction of CDKIs and cell cycle arrest, whereas transient activation promotes cell cycle.

This cellular activation model provides a possible explanation for the accumulation of activated/memory phenotype $CD4^+$ T cells in lupus (Fig. 7). We hypothesize that genetic susceptibility predisposes lupus T cells to hyperrespond through a variety of mechanisms, such as increased antigen presentation or lack of regulatory signaling. Many of these mechanisms have been revealed recently by analyses of spontaneous as well as gene knockout and transgenic mice with lupuslike disease (46, 47). This enhanced activa-

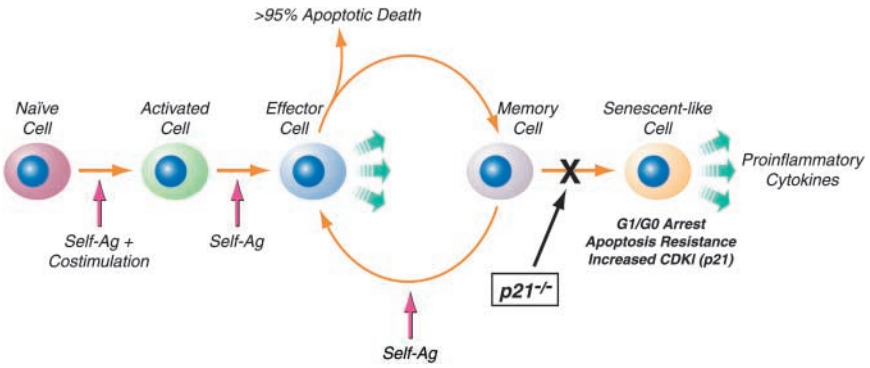

Figure 7. T cell senescence and p21 in systemic autoimmunity. In lupus-prone mice, the accumulated activated/memory $CD4^+$ T cells are in a state resembling replicative senescence. We hypothesize that repeated stimulation of $CD4^+$ T cells (depicted by the hypothetical movement of cells from the memory to effector compartments) by self-antigens (Ag) leads to resistance to proliferation and apoptosis (senescent-like cell), due in large part to increased levels of CDKIs. Senescent cells are metabolically active and can produce proinflammatory cytokines. As shown in this work, the gradual accumulation of these activated/memory phenotype $CD4^+$ T cells and subsequent development of autoimmunity is dependent on p21. Furthermore, our data indicate that the fraction of activated/memory $CD4^+CD44^{hi}$ T cells that escape AICD in wild-type autoimmune mice (because of increased CDKIs) do not accumulate in G_0/G_1-phase in p21-deficient mice; instead, they proliferate and become susceptible to Fas-mediated apoptosis. Thus, the lack of p21 appears to restore homeostasis of autoreactive $CD4^+CD44^{hi}$ T cells by preventing their transition to a senescent-like state.

tion, together with continuous stimulation by ever-present self-antigens, will lead to repeated interconversions of T cells from effector to memory and vice versa. Selection of high affinity memory T cells results in increased MAPK signaling, induction of CDKIs, and finally accumulation of memory phenotype T cells that are replication and apoptosis resistant. Potential experimental analogies are resistance to cell cycle progression of T cells cultured for prolonged periods with anti-CD3 antibody (48) and high concentrations of superantigen (49) or specific antigen (50). In further support of this hypothesis, HLA-A1–specific T cells repeatedly stimulated in vitro with antigen to emulate possible autoimmune responses converted to effector/memory phenotype cells resistant to CD95-mediated AICD (51). As discussed here, absence of the pancyclin inhibitor p21 reduces the likelihood of cells attaining this G_0/G_1 arrested state, and their accumulation. It is significant that despite the multiple pancyclin inhibitors (p21, p27, and p57), deletion of p21 can accomplish this effect, implying that functional redundancy among these molecules is only partial.

Extensive data have shown previously that p21 inhibits apoptosis of various cell types by directly affecting expression/function of several molecules involved in this process (24, 52). We demonstrated that p21 deletion amplified T cell AICD by promoting the extrinsic pathway of apoptosis. Thus, in the absence of p21, Fas/FasL-mediated apoptosis was enhanced, concurrent with increased conversion of procaspases 8 and 3 to active caspases, and loss of mitochondrial transmembrane potential. Moreover, wild-type T cells behaved similarly to p21-deficient cells when transfected with p21 AS oligonucleotides. The results clearly establish that p21 is a significant inhibitor of Fas/FasL-mediated T cell apoptosis. Enhanced sensitization of glioma cells to CD95-mediated apoptosis with p21 AS oligonucleotides associated with increased caspase 8 and 3 activation has been shown previously (40). We also observed increased apoptosis of anti-IgM cross-linked $p21^{-/-}$ B cells, in agreement with studies showing diminished G_1-arrest and increased apoptosis of B cells treated with p21 AS oligonucleotides (53).

A potential biochemical explanation for the increased activation of procaspase 3 may be provided by the series of observations by Suzuki et al., who reported that p21 released from the CDK4/6 complex by survivin translocates to the mitochondria, binds to a putative mitochondrial adaptor protein, and sequesters procaspase 3 (54–57). Moreover, because p21 binds to the cleavage site of procaspase 3, conversion to the p17 active fragment is also reduced, thus impeding Fas-mediated apoptosis. In addition, evidence has been presented that active caspase 3 can cleave p21, reducing its inhibitory effects and accelerating apoptosis (58–61). Increases in proximal caspase 8 activation of p21-deficient cells undergoing AICD might be attributed to less interference with procaspase 8 cleavage (24), or to a feedback effect mediated by the increased levels of activated caspase 3 (40).

Depending on cell type and/or signal intensity, the extrinsic and intrinsic pathways of apoptosis may converge (38, 39). We found that activated $p21^{-/-}$ T cells had only a moderate increase in p53 levels and a slight shift in the ratio of Bax/Bcl-2 toward the proapoptotic Bax. Stabilization of p53 and inversion of the Bcl-2/Bax ratio has also been reported in carcinoma cells undergoing chemotherapeutic drug-induced apoptosis (62). However, it appears that the intrinsic pathway plays a minor role, if any, in the enhanced AICD of $p21^{-/-}$ T cells.

A slight reduction in the percentage (7.8 vs. 12.2%) of quiescent G_0-phase hematopoietic stem cells in $p21^{-/-}$ BXSB mice was also observed. However, this was not associated with hematopoietic precursor insufficiency, consistent with a previous paper in which $p21^{-/-}$ bone marrow cells that required three serial passages before significant stem cell deficiency was observed (30). Furthermore, the reduction of T and B cells was limited to only certain lymphoid organs and cell subsets. Thus, it is highly unlikely that the slight decrease in percentage of quiescent stem cells plays a significant role in the reduction in activated/memory T and B cells and autoimmune disease in $p21^{-/-}$ mice.

One of the most striking findings in this work is the difference in TD antibody responses of $p21^{-/-}$ and wild-type BXSB mice. In the primary response, $p21^{-/-}$ mice showed

much higher IgG levels, whereas in the secondary response, the antibody levels declined more rapidly compared with wild-type mice. The enhanced primary antibody response in $p21^{-/-}$ mice is likely due to accelerated proliferation of helper T cells, whereas the rapid reduction in the secondary response is likely caused by increased AICD. This finding is compatible with our hypothesis that, under conditions of sustained T cell stimulation by constant exposure to self-antigens, lack of p21 leads to enhanced proliferation and apoptosis of self-reactive helper T cells, thereby reducing autoantibody responses.

Our findings contrast sharply with an initial report that older female, but not male, $p21^{-/-}$ mice of mixed 129/Sv × C57BL/6 (129 × B6) background develop severe lupuslike features (36). Subsequent analyses by us with a different group of $p21^{-/-}$ mixed-background 129 × B6 mice and, more significantly, with female BXSB $p21^{-/-}$ mice containing all lupus-predisposing genes except the *Yaa*, showed no appreciable induction of autoimmune disease (34, 37). Several papers have documented that the 129 × B6 mixed genomes spontaneously develop signs of systemic autoimmunity with low levels of GN, especially in females of advanced age (37, 63–66). Therefore, systemic autoimmunity in gene-deleted 129 × B6 mice should be carefully controlled by performing a sufficient number of backcrosses to attain genetic homogeneity, and should include wild-type littermates. The present paper makes it clear that modulation of the cell cycle pathway by deleting the CDKI p21 inhibits the development of systemic autoimmunity. This is further supported by our recent finding that deficiency in another CDKI (i.e., p27) also results in reduction of lupuslike disease in male BXSB mice (unpublished data).

Although our work focused on male BXSB lupus mice, expansion of activated/memory phenotype T cell populations is common to other lupus strains (5, 67), and is observed in human systemic lupus erythematosus (68, 69). Accumulation of G_0/G_1-arrested T cell populations has also been observed in other autoimmune diseases, such as rheumatoid arthritis (70) and insulin-dependent diabetes (71, 72), and even in aging (73), suggesting that these cells may also contribute to the pathogenesis of these diseases and to immune senescence.

The present paper raises the possibility that efforts to block the activity of CDKIs may be a means to intervene in systemic autoimmunity and other immune-related disorders. The primary contribution of p21 in disease pathogenesis, and the relatively benign consequences of p21 deficiency (24), makes it a particularly promising therapeutic target. Blockade of p21 and possibly other CDKIs could be a novel approach that, instead of inhibiting, promotes proliferation and hence apoptosis of the accumulated autoreactive T and B cells. This may be a particularly powerful strategy for eliminating disease-promoting cells in advanced autoimmune diseases.

We thank J.D. Kuan, L. Simpson, V. Clifton, S. Koundouris, and A. Szydlik for their technical assistance, M.K. Occhipinti and J. Kuhns for their editorial assistance, and Drs. J. Sprent, G. Bokoch, and S. Reed for manuscript review and comments.

This is publication number 14384-IMM from the Department of Immunology at the The Scripps Research Institute. The work herein was supported in part by U.S. Public Health Service grants AR32103, AG15061, AR39555, and AR42242, and National Institutes of Health training grant AG00080.

Submitted: 30 September 2003
Accepted: 18 December 2003

References

1. Sprent, J., and D.F. Tough. 1994. Lymphocyte life-span and memory. *Science.* 265:1395–1400.
2. Ahmed, R., and D. Gray. 1996. Immunological memory and protective immunity: understanding their relation. *Science.* 272:54–60.
3. Theofilopoulos, A.N., and D.H. Kono. 1999. Murine lupus models: gene-specific and genome-wide studies. *In* Systemic Lupus Erythematosus. R.G. Lahita, editor. Academic Press, San Diego. 145–181.
4. Chu, E.B., D.N. Ernst, M.V. Hobbs, and W.O. Weigle. 1994. Maturational changes in CD4+ cell subsets and lymphokine production in BXSB mice. *J. Immunol.* 152:4129–4138.
5. Sabzevari, H., S. Propp, D.H. Kono, and A.N. Theofilopoulos. 1997. G1 arrest and high expression of cyclin kinase and apoptosis inhibitors in accumulated activated/memory phenotype CD4+ cells of older lupus mice. *Eur. J. Immunol.* 27: 1901–1910.
6. Campisi, J. 1996. Replicative senescence: an old lives' tale? *Cell.* 84:497–500.
7. Noda, A., Y. Ning, S.F. Venable, O.M. Pereira-Smith, and J.R. Smith. 1994. Cloning of senescent cell-derived inhibitors of DNA synthesis using an expression screen. *Exp. Cell Res.* 211:90–98.
8. Sayama, K., Y. Shirakata, K. Midorikawa, Y. Hanakawa, and K. Hashimoto. 1999. Possible involvement of p21 but not of p16 or p53 in keratinocyte senescence. *J. Cell. Physiol.* 179:40–44.
9. Prud'homme, G.J., D.H. Kono, and A.N. Theofilopoulos. 1995. Quantitative polymerase chain reaction analysis reveals marked overexpression of interleukin-1β, interleukin-1 and interferon-γ mRNA in the lymph nodes of lupus-prone mice. *Mol. Immunol.* 32:495–503.
10. Kozono, Y., B.L. Kotzin, and V.M. Holers. 1996. Resting B cells from New Zealand Black mice demonstrate a defect in apoptosis induction following surface IgM ligation. *J. Immunol.* 156:4498–4503.
11. Wither, J.E., A.D. Paterson, and B. Vukusic. 2000. Genetic dissection of B cell traits in New Zealand black mice. The expanded population of B cells expressing up-regulated costimulatory molecules shows linkage to Nba2. *Eur. J. Immunol.* 30:356–365.
12. Blossom, S., E.B. Chu, W.O. Weigle, and K.M. Gilbert. 1997. CD40 ligand expressed on B cells in the BXSB mouse model of systemic lupus erythematosus. *J. Immunol.* 159: 4580–4586.
13. Theofilopoulos, A.N., and F.J. Dixon. 1985. Murine models of systemic lupus erythematosus. *Adv. Immunol.* 37:269–390.
14. Green, D.R., and D.W. Scott. 1994. Activation-induced apoptosis in lymphocytes. *Curr. Opin. Immunol.* 6:476–487.
15. Sherr, C.J. 1996. Cancer cell cycles. *Science.* 274:1672–1677.
16. Renno, T., A. Attinger, S. Locatelli, T. Bakker, S. Vacheron, and H.R. MacDonald. 1999. Cutting edge: apoptosis of super-

antigen-activated T cells occurs preferentially after a discrete number of cell divisions in vivo. *J. Immunol.* 162:6312–6315.
17. Boehme, S.A., and M.J. Lenardo. 1993. Propriocidal apoptosis of mature T lymphocytes occurs at S phase of the cell cycle. *Eur. J. Immunol.* 23:1552–1560.
18. Radvanyi, L.G., Y. Shi, G.B. Mills, and R.G. Miller. 1996. Cell cycle progression out of G1 sensitizes primary-cultured nontransformed T cells to TCR-mediated apoptosis. *Cell. Immunol.* 170:260–273.
19. Fotedar, R., J. Flatt, S. Gupta, R.L. Margolis, P. Fitzgerald, H. Messier, and A. Fotedar. 1995. Activation-induced T-cell death is cell cycle dependent and regulated by cyclin B. *Mol. Cell. Biol.* 15:932–942.
20. Sherr, C.J., and J.M. Roberts. 1999. CDK inhibitors: positive and negative regulators of G1-phase progression. *Genes Dev.* 13:1501–1512.
21. Dotto, G.P. 2000. p21(WAF1/Cip1): more than a break to the cell cycle? *Biochim. Biophys. Acta.* 1471:M43–M56.
22. Harada, K., and G.R. Ogden. 2000. An overview of the cell cycle arrest protein, p21(WAF1). *Oral Oncol.* 36:3–7.
23. Vousden, K.H. 2000. p53: death star. *Cell.* 103:691–694.
24. Gartel, A.L., and A.L. Tyner. 2002. The role of the cyclin-dependent kinase inhibitor p21 in apoptosis. *Mol. Cancer Ther.* 1:639–649.
25. Hobeika, A.C., W. Etienne, B.A. Torres, H.M. Johnson, and P.S. Subramaniam. 1999. IFN-gamma induction of p21(WAF1) is required for cell cycle inhibition and suppression of apoptosis. *J. Interferon Cytokine Res.* 19:1351–1361.
26. Xaus, J., M. Cardo, A.F. Valledor, C. Soler, J. Lloberas, and A. Celada. 1999. Interferon gamma induces the expression of p21waf-1 and arrests macrophage cell cycle, preventing induction of apoptosis. *Immunity.* 11:103–113.
27. Deng, C., P. Zhang, J.W. Harper, S.J. Elledge, and P. Leder. 1995. Mice lacking p21CIP1/WAF1 undergo normal development, but are defective in G1 checkpoint control. *Cell.* 82: 675–684.
28. Le, L.Q., J.H. Kabarowski, Z. Weng, A.B. Satterthwaite, E.T. Harvill, E.R. Jensen, J.F. Miller, and O.N. Witte. 2001. Mice lacking the orphan G protein-coupled receptor G2A develop a late-onset autoimmune syndrome. *Immunity.* 14: 561–571.
29. Lawson, B.R., G.J. Prud'homme, Y. Chang, H.A. Gardner, J. Kuan, D.H. Kono, and A.N. Theofilopoulos. 2000. Treatment of murine lupus with cDNA encoding IFN-γR/Fc. *J. Clin. Invest.* 106:207–215.
30. Cheng, T., N. Rodrigues, H. Shen, Y. Yang, D. Dombkowski, M. Sykes, and D.T. Scadden. 2000. Hematopoietic stem cell quiescence maintained by p21cip1/waf1. *Science.* 287:1804–1808.
31. Okahashi, N., Y. Murase, T. Koseki, T. Sato, K. Yamato, and T. Nishihara. 2001. Osteoclast differentiation is associated with transient upregulation of cyclin-dependent kinase inhibitors p21(WAF1/CIP1) and p27(KIP1). *J. Cell. Biochem.* 80:339–345.
32. Fujio, Y., K. Guo, T. Mano, Y. Mitsuuchi, J.R. Testa, and K. Walsh. 1999. Cell cycle withdrawal promotes myogenic induction of Akt, a positive modulator of myocyte survival. *Mol. Cell. Biol.* 19:5073–5082.
33. Park, C.L., R.S. Balderas, T.M. Fieser, J.H. Slack, G.J. Prud'Homme, F.J. Dixon, and A.N. Theofilopoulos. 1983. Isotypic profiles and other fine characteristics of immune responses to exogenous thymus-dependent and -independent antigens by mice with lupus syndromes. *J. Immunol.* 130: 2161–2167.
34. Lawson, B.R., D.H. Kono, and A.N. Theofilopoulos. 2002. Deletion of p21 (WAF-1/Cip1) does not induce systemic autoimmunity in female BXSB mice. *J. Immunol.* 168:5928–5932.
35. Wofsy, D., C.E. Kerger, and W.E. Seaman. 1984. Monocytosis in the BXSB model for systemic lupus erythematosus. *J. Exp. Med.* 159:629–634.
36. Balomenos, D., J. Martin-Caballero, M.I. Garcia, I. Prieto, J.M. Flores, M. Serrano, and A.C. Martinez. 2000. The cell cycle inhibitor p21 controls T-cell proliferation and sex-linked lupus development. *Nat. Med.* 6:171–176.
37. Santiago-Raber, M.L., B.R. Lawson, W. Dummer, M. Barnhouse, S. Koundouris, C.B. Wilson, D.H. Kono, and A.N. Theofilopoulos. 2001. Role of cyclin kinase inhibitor p21 in systemic autoimmunity. *J. Immunol.* 167:4067–4074.
38. Hengartner, M.O. 2000. The biochemistry of apoptosis. *Nature.* 407:770–776.
39. Krammer, P.H. 2000. CD95's deadly mission in the immune system. *Nature.* 407:789–795.
40. Glaser, T., B. Wagenknecht, and M. Weller. 2001. Identification of p21 as a target of cycloheximide-mediated facilitation of CD95-mediated apoptosis in human malignant glioma cells. *Oncogene.* 20:4757–4767.
41. Blossom, S.J., and K.M. Gilbert. 2000. B cells from autoimmune BXSB mice are hyporesponsive to signals provided by CD4+ T cells. *Immunol. Invest.* 29:287–297.
42. Blagosklonny, M.V. 2003. Cell senescence and hypermitogenic arrest. *EMBO Rep.* 4:358–362.
43. Marshall, C.J. 1995. Specificity of receptor tyrosine kinase signaling: transient versus sustained extracellular signal-regulated kinase activation. *Cell.* 80:179–185.
44. Woods, D., D. Parry, H. Cherwinski, E. Bosch, E. Lees, and M. McMahon. 1997. Raf-induced proliferation or cell cycle arrest is determined by the level of Raf activity with arrest mediated by p21Cip1. *Mol. Cell. Biol.* 17:5598–5611.
45. Sewing, A., B. Wiseman, A.C. Lloyd, and H. Land. 1997. High-intensity Raf signal causes cell cycle arrest mediated by p21Cip1. *Mol. Cell. Biol.* 17:5588–5597.
46. Kono, D.H., R. Baccala, and A.N. Theofilopoulos. 2004. Genes and genetics of murine lupus. *In* Systemic Lupus Erythematosus. R.G. Lahita, editor. Academic Press, San Diego. In press.
47. Vratsanos, G.S., S. Jung, Y.M. Park, and J. Craft. 2001. CD4(+) T cells from lupus-prone mice are hyperresponsive to T cell receptor engagement with low and high affinity peptide antigens: a model to explain spontaneous T cell activation in lupus. *J. Exp. Med.* 193:329–337.
48. Andris, F., M. Van Mechelen, F. De Mattia, E. Baus, J. Urbain, and O. Leo. 1996. Induction of T cell unresponsiveness by anti-CD3 antibodies occurs independently of co-stimulatory functions. *Eur. J. Immunol.* 26:1187–1195.
49. Miethke, T., C. Wahl, H. Gaus, K. Heeg, and H. Wagner. 1994. Exogenous superantigens acutely trigger distinct levels of peripheral T cell tolerance/immunosuppression: dose–response relationship. *Eur. J. Immunol.* 24:1893–1902.
50. Gilbert, K.M., and W.O. Weigle. 1993. Th1 cell anergy and blockade in G1a phase of the cell cycle. *J. Immunol.* 151: 1245–1254.
51. Strauss, G., I. Knape, I. Melzner, and K.M. Debatin. 2003. Constitutive caspase activation and impaired death-inducing signaling complex formation in CD95-resistant, long-term activated, antigen-specific T cells. *J. Immunol.* 171:1172–1182.
52. Poluha, W., D.K. Poluha, B. Chang, N.E. Crosbie, C.M.

Schonhoff, D.L. Kilpatrick, and A.H. Ross. 1996. The cyclin-dependent kinase inhibitor p21 (WAF1) is required for survival of differentiating neuroblastoma cells. *Mol. Cell. Biol.* 16:1335–1341.
53. Marches, R., R. Hsueh, and J.W. Uhr. 1999. Cancer dormancy and cell signaling: induction of p21(waf1) initiated by membrane IgM engagement increases survival of B lymphoma cells. *Proc. Natl. Acad. Sci. USA.* 96:8711–8715.
54. Suzuki, A., Y. Tsutomi, K. Akahane, T. Araki, and M. Miura. 1998. Resistance to Fas-mediated apoptosis: activation of caspase 3 is regulated by cell cycle regulator p21WAF1 and IAP gene family ILP. *Oncogene.* 17:931–939.
55. Suzuki, A., Y. Tsutomi, M. Miura, and K. Akahane. 1999. Caspase 3 inactivation to suppress Fas-mediated apoptosis: identification of binding domain with p21 and ILP and inactivation machinery by p21. *Oncogene.* 18:1239–1244.
56. Suzuki, A., Y. Tsutomi, N. Yamamoto, T. Shibutani, and K. Akahane. 1999. Mitochondrial regulation of cell death: mitochondria are essential for procaspase 3-p21 complex formation to resist Fas-mediated cell death. *Mol. Cell. Biol.* 19:3842–3847.
57. Suzuki, A., T. Ito, H. Kawano, M. Hayashida, Y. Hayasaki, Y. Tsutomi, K. Akahane, T. Nakano, M. Miura, and K. Shiraki. 2000. Survivin initiates procaspase 3/p21 complex formation as a result of interaction with Cdk4 to resist Fas-mediated cell death. *Oncogene.* 19:1346–1353.
58. Gervais, J.L., P. Seth, and H. Zhang. 1998. Cleavage of CDK inhibitor p21(Cip1/Waf1) by caspases is an early event during DNA damage-induced apoptosis. *J. Biol. Chem.* 273: 19207–19212.
59. Levkau, B., H. Koyama, E.W. Raines, B.E. Clurman, B. Herren, K. Orth, J.M. Roberts, and R. Ross. 1998. Cleavage of p21Cip1/Waf1 and p27Kip1 mediates apoptosis in endothelial cells through activation of Cdk2: role of a caspase cascade. *Mol. Cell.* 1:553–563.
60. Park, J.A., K.W. Kim, S.I. Kim, and S.K. Lee. 1998. Caspase 3 specifically cleaves p21WAF1/CIP1 in the earlier stage of apoptosis in SK-HEP-1 human hepatoma cells. *Eur. J. Biochem.* 257:242–248.
61. Zhang, Y., N. Fujita, and T. Tsuruo. 1999. Caspase-mediated cleavage of p21Waf1/Cip1 converts cancer cells from growth arrest to undergoing apoptosis. *Oncogene.* 18:1131–1138.
62. Javelaud, D., and F. Besancon. 2002. Inactivation of p21WAF1 sensitizes cells to apoptosis via an increase of both p14ARF and p53 levels and an alteration of the Bax/Bcl-2 ratio. *J. Biol. Chem.* 277:37949–37954.
63. Botto, M., C. Dell'Agnola, A.E. Bygrave, E.M. Thompson, H.T. Cook, F. Petry, M. Loos, P.P. Pandolfi, and M.J. Walport. 1998. Homozygous C1q deficiency causes glomerulonephritis associated with multiple apoptotic bodies. *Nat. Genet.* 19:56–59.
64. Bickerstaff, M.C., M. Botto, W.L. Hutchinson, J. Herbert, G.A. Tennent, A. Bybee, D.A. Mitchell, H.T. Cook, P.J. Butler, M.J. Walport, and M.B. Pepys. 1999. Serum amyloid P component controls chromatin degradation and prevents antinuclear autoimmunity. *Nat. Med.* 5:694–697.
65. Wakeland, E.K., K. Liu, R.R. Graham, and T.W. Behrens. 2001. Delineating the genetic basis of systemic lupus erythematosus. *Immunity.* 15:397–408.
66. Mitchell, D.A., M.C. Pickering, J. Warren, L. Fossati-Jimack, J. Cortes-Hernandez, H.T. Cook, M. Botto, and M.J. Walport. 2002. C1q deficiency and autoimmunity: the effects of genetic background on disease expression. *J. Immunol.* 168:2538–2543.
67. Balomenos, D., R. Rumold, and A.N. Theofilopoulos. 1997. The proliferative in vivo activities of lpr double-negative T cells and the primary role of p59fyn in their activation and expansion. *J. Immunol.* 159:2265–2273.
68. Gmelig-Meyling, F., S. Dawisha, and A.D. Steinberg. 1992. Assessment of in vivo frequency of mutated T cells in patients with systemic lupus erythematosus. *J. Exp. Med.* 175:297–300.
69. Dayal, A.K., and G.M. Kammer. 1996. The T cell enigma in lupus. *Arthritis Rheum.* 39:23–33.
70. Goronzy, J.J., and C.M. Weyand. 2001. Thymic function and peripheral T-cell homeostasis in rheumatoid arthritis. *Trends Immunol.* 22:251–255.
71. Petersen, L.D., G. Duinkerken, G.J. Bruining, R.A. van Lier, R.R. de Vries, and B.O. Roep. 1996. Increased numbers of in vivo activated T cells in patients with recent onset insulin-dependent diabetes mellitus. *J. Autoimmun.* 9:731–737.
72. Smerdon, R.A., M. Peakman, M.J. Hussain, L. Alviggi, P.J. Watkins, R.D. Leslie, and D. Vergani. 1993. Increase in simultaneous coexpression of naive and memory lymphocyte markers at diagnosis of IDDM. *Diabetes.* 42:127–133.
73. Arbogast, A., S. Boutet, M.A. Phelouzat, O. Plastre, R. Quadri, and J.J. Proust. 1999. Failure of T lymphocytes from elderly humans to enter the cell cycle is associated with low Cdk6 activity and impaired phosphorylation of Rb protein. *Cell. Immunol.* 197:46–54.